nature portfolio

https://doi.org/10.1038/s41562-021-01099-4

Supplementary information

Different computations underlie overt presaccadic and covert spatial attention

In the format provided by the authors and unedited

Supplementary Information for Different computations underlie overt presaccadic and covert spatial attention

Hsin-Hung Li, Jasmine Pan and Marisa Carrasco

Supplementary Figures

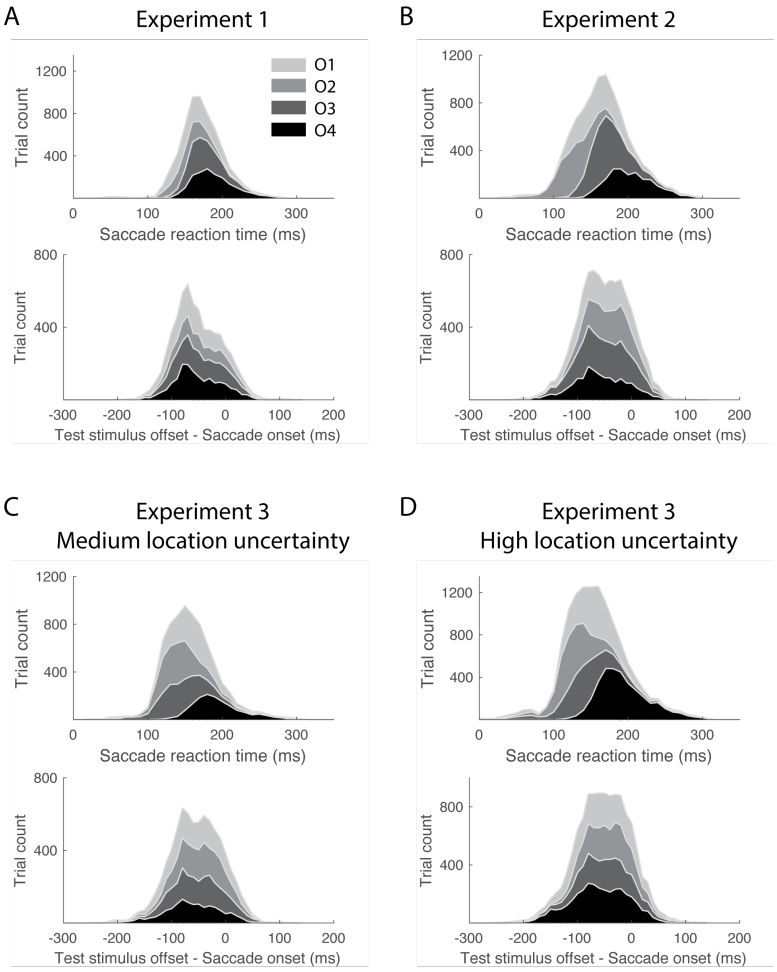

Supplementary Figure 1. Distribution of saccade reaction time (saccade onset minus saccade cue onset) and latency (test stimulus offset minus saccade onset). Four different shades of gray are used to indicate the four different observers (O1 to O4) **(A)** Experiment 1. **(B)** Experiment 2. **(C)** Experiment 3, Medium location uncertainty condition. **(D)** Experiment 3, High location uncertainty condition. In all the figures, the distributions from different observers are stacked.

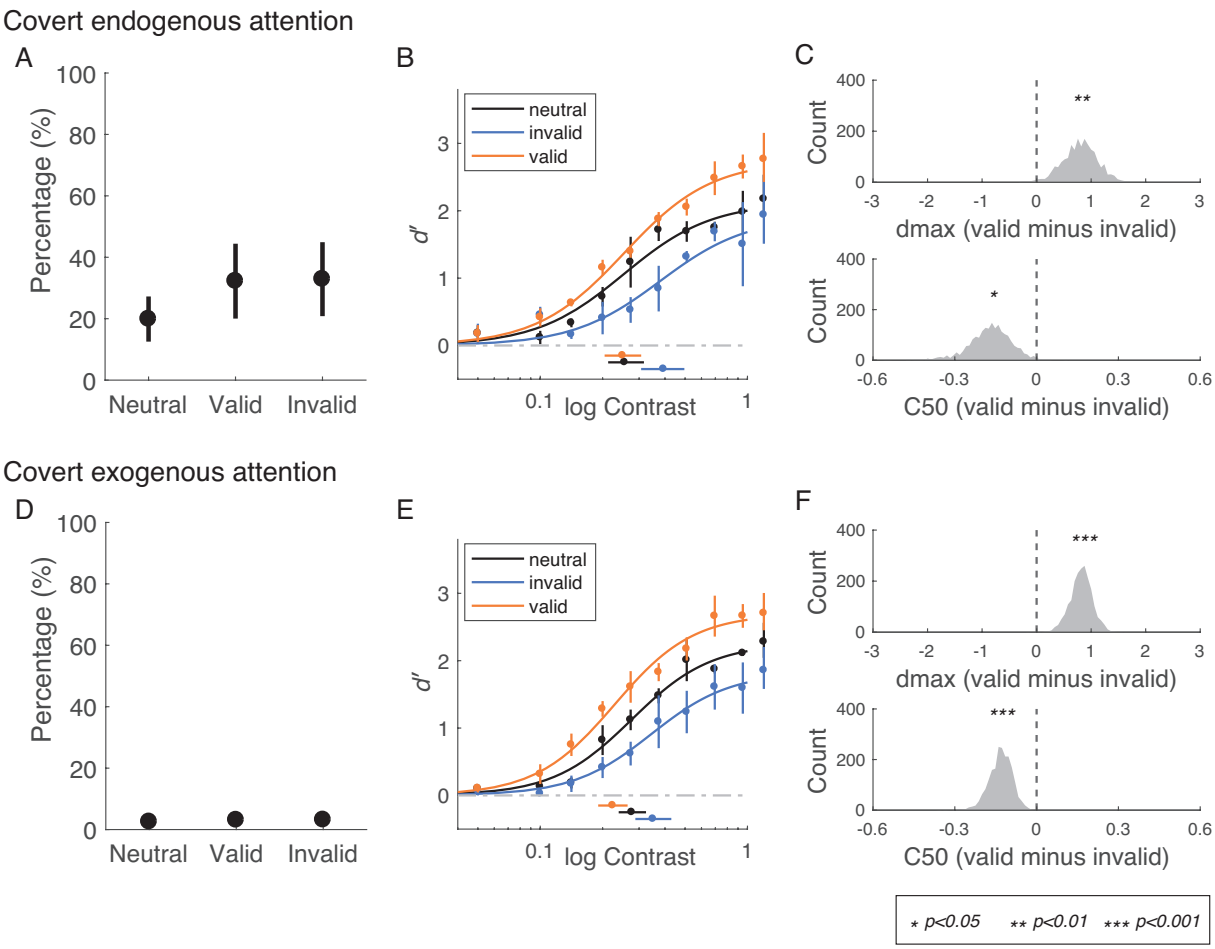

Supplementary Figure 2. Effects of covert attention without fixational eye movements. (**A-C**) Covert endogenous attention condition. (**A**) Percentage of trials that contain fixational eye movement during the critical interval (from the pre-cue onset to the stimulus onset) in the neutral, valid and invalid conditions. (**B**) Group-averaged psychometric functions (d′ vs. contrast) for the trials without fixational eye movements during the critical interval. The error bars represent 95% bootstrapped confidence interval. (**C**) The bootstrapped distribution of the difference of d_{max} (top) and the difference of C50 (bottom) between the Toward and Away conditions. The distributions significantly different from zero are denoted with asterisks. (**D-F**) covert exogenous attention condition.

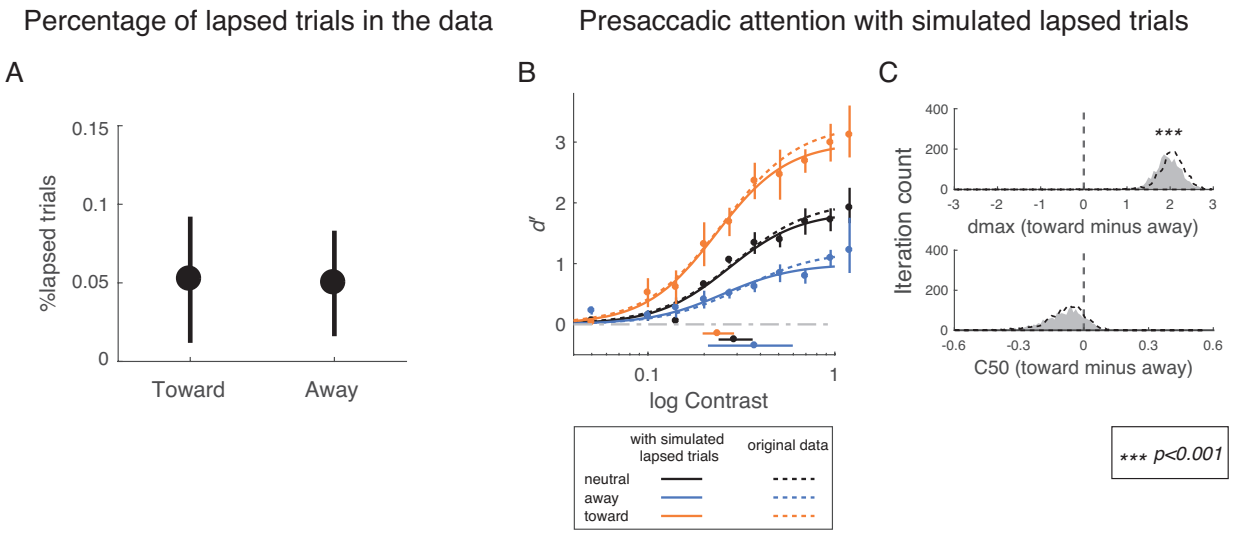

Supplementary Figure 3. **Presaccadic attention effect with simulated lapsed responses**. (A) Percentage of the lapsed trials in the Toward and Away conditions. See Methods for the definition of lapsed trials. (**B**) Group-averaged psychometric functions (d′ vs. contrast) with simulated lapsed responses. d_{max} and C_{50} of the group-averaged psychometric functions are plotted at the right and the bottom of the figure. The error bars represent 95% bootstrapped confidence interval. The dashed lines denote the original data (without simulated lapsed trials) plotted in Figure 4. (The neutral condition also contained some lapsed trials in which blinks occurred upon stimulus presentation). (**C**) The bootstrapped distribution of the difference of d_{max} (top) and the difference of C50 (bottom) between the Toward and Away conditions. The distribution significant different from zero is denoted with asterisks. The distributions outlined by the dashed curves denote the original data (without simulated lapsed trials) plotted in Figure 4.

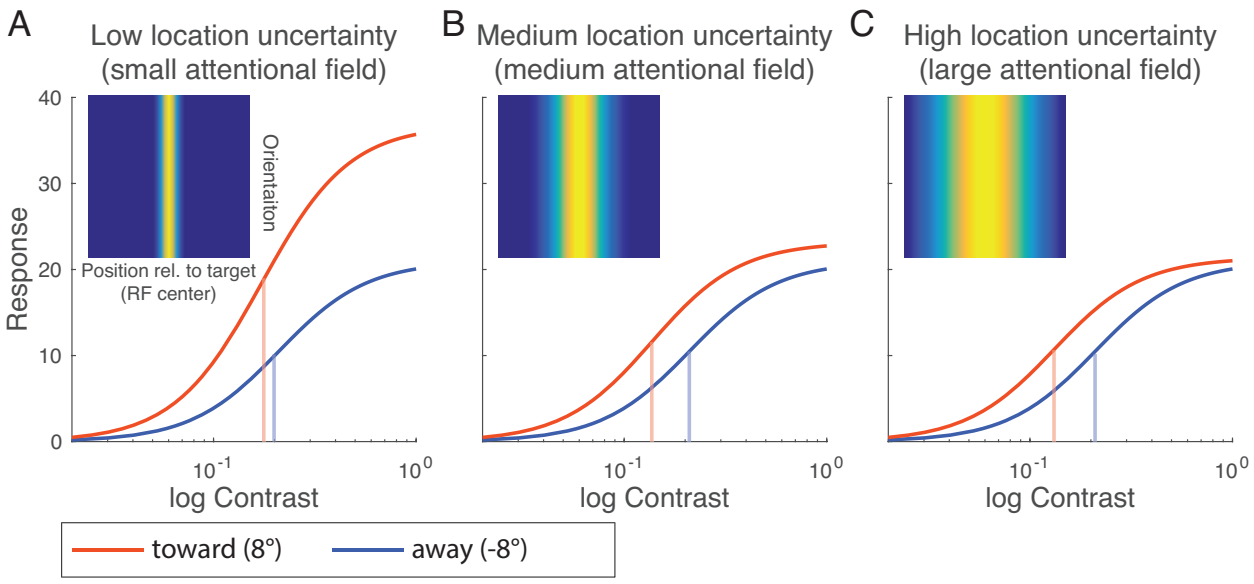

Supplementary Figure 4. Simulations. Neural responses were simulated based on the Normalization Model of Attention (Reynolds and Heeger, 2009; see NMA in Models in Methods). (**A**) Simulated neural response as a function of stimulus contrast in the low-uncertainty condition. The vertical lines indicate the semi-saturation contrast of the contrast response functions. The figure legend indicates the attentional gain factor in this condition. The inset is the attentional gain factors used for simulating the Toward condition. The attentional gain factors were set at the baseline (=1, equivalent to the dark blue color in the inset) across the entire neural population for the Away condition. (**B**) Medium location uncertainty condition. (**C**) High location uncertainty condition.

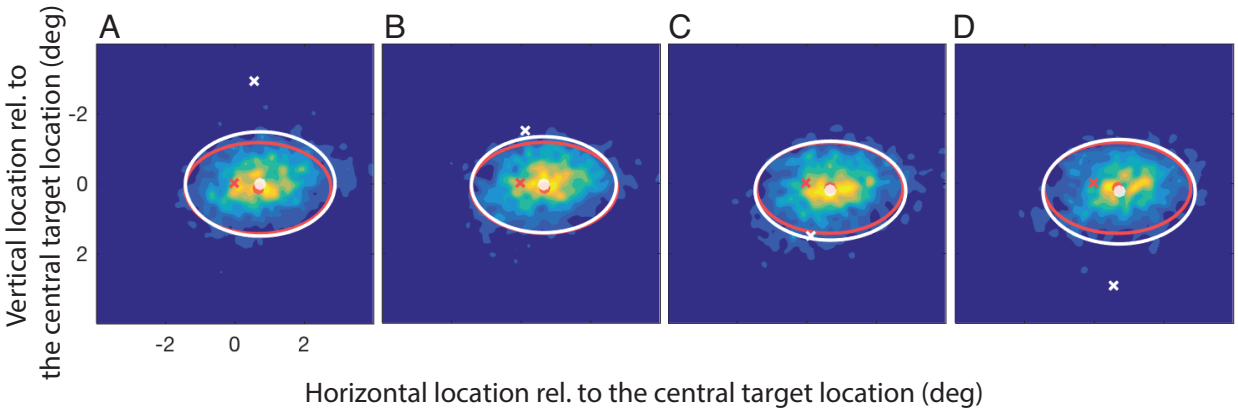

Supplementary Figure 5. **Distributions of saccade landing positions in the high-uncertainty condition in Experiment 3.** We collapse leftward and rightward saccades by flipping the sign of the horizontal location of the saccade landing points of all the rightward saccades. Distributions of saccade landing points were first computed for each observer and then averaged across all observers. In all the figures, we compared the distribution of the saccade landing positions when the target was presented at the off-center locations with the distribution when the target was presented at the central location. In all the figures, the red cross is the location of the central target, and the red ellipse and the red dot represent the distribution of saccade landing positions when the target was presented at the central location. (**A**) The background color represents the distribution of saccade landing positions when the target was presented at the topmost position (denoted by the white cross). This distribution is further illustrated by the white ellipse: The center of the white ellipse is the mean of the distribution (denoted by the white dot), and the axes of the white ellipse represent ±standard deviation along horizontal and vertical directions. (**B**-**D**) In the same format as (**A**), the distributions of saccade landing points when the target was presented at the other three off-center locations were illustrated by the background color and all the white symbols.

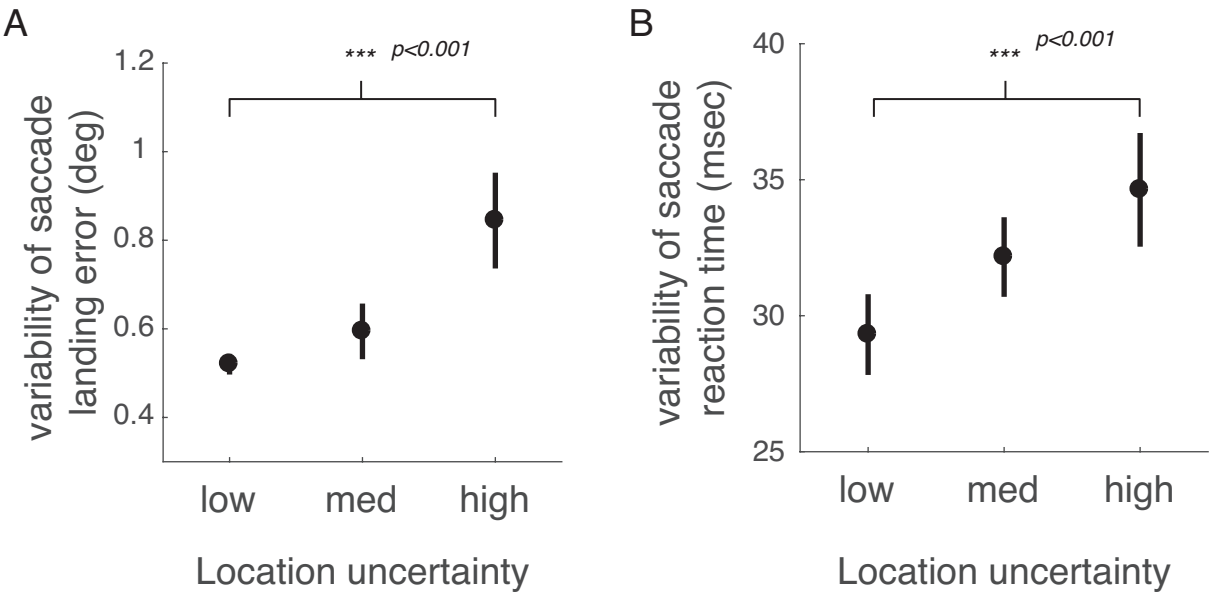

Supplementary Figure 6. Effects of location uncertainty on oculomotor behaviors. (**A**) The variability of saccade landing error as a function of location uncertainty. (**B**) The variability of saccade reaction time as a function of location uncertainty. In both cases, the variability increased with location uncertainty.

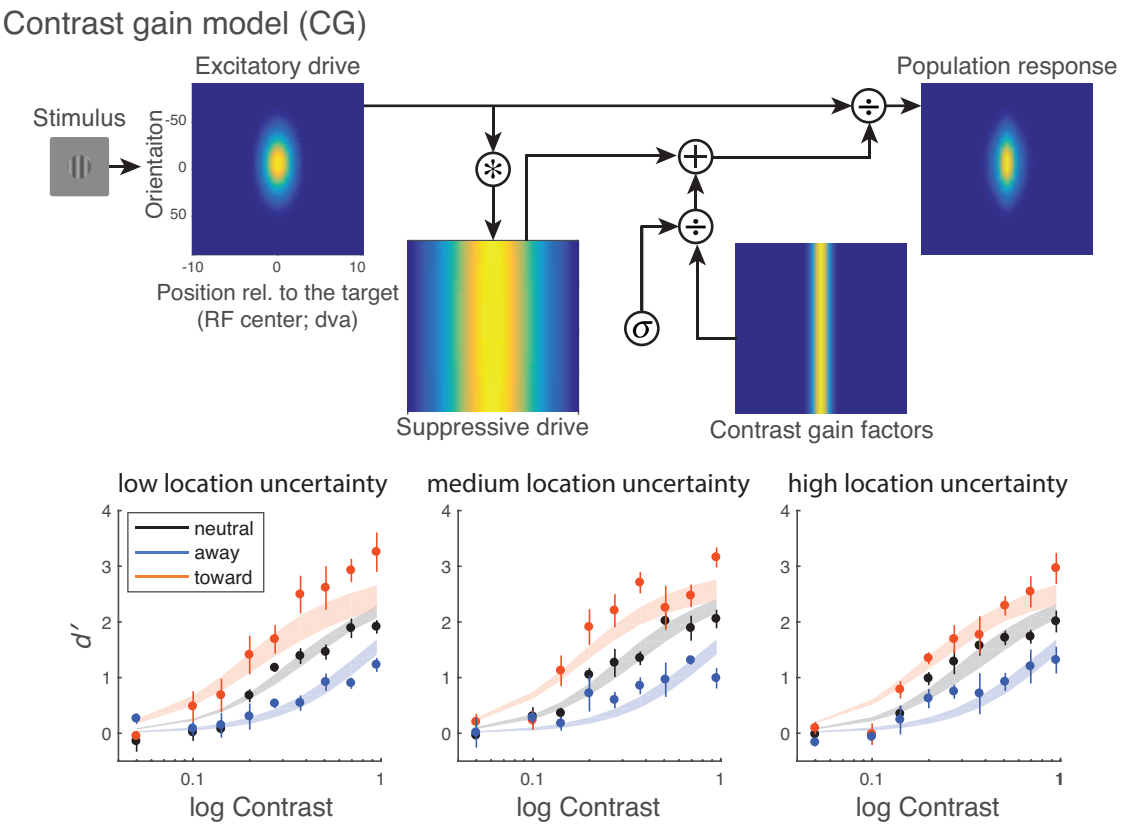

Supplementary Figure 7. **Contrast gain model and model fit.** Top row: Contrast gain model. Attention modulates the suppression constant (σ) of the neurons divisively. Note that the suppression constant is present in all the models, but for simplicity, it is not shown in the figures of other models. Bottom row: Model fit. Data points and error bars represent group-averaged data and ±1 s.e.m. The model was fitted to individual observers, and the shading areas represent the averaged of the fit across observers (mean ±1 s.e.m).

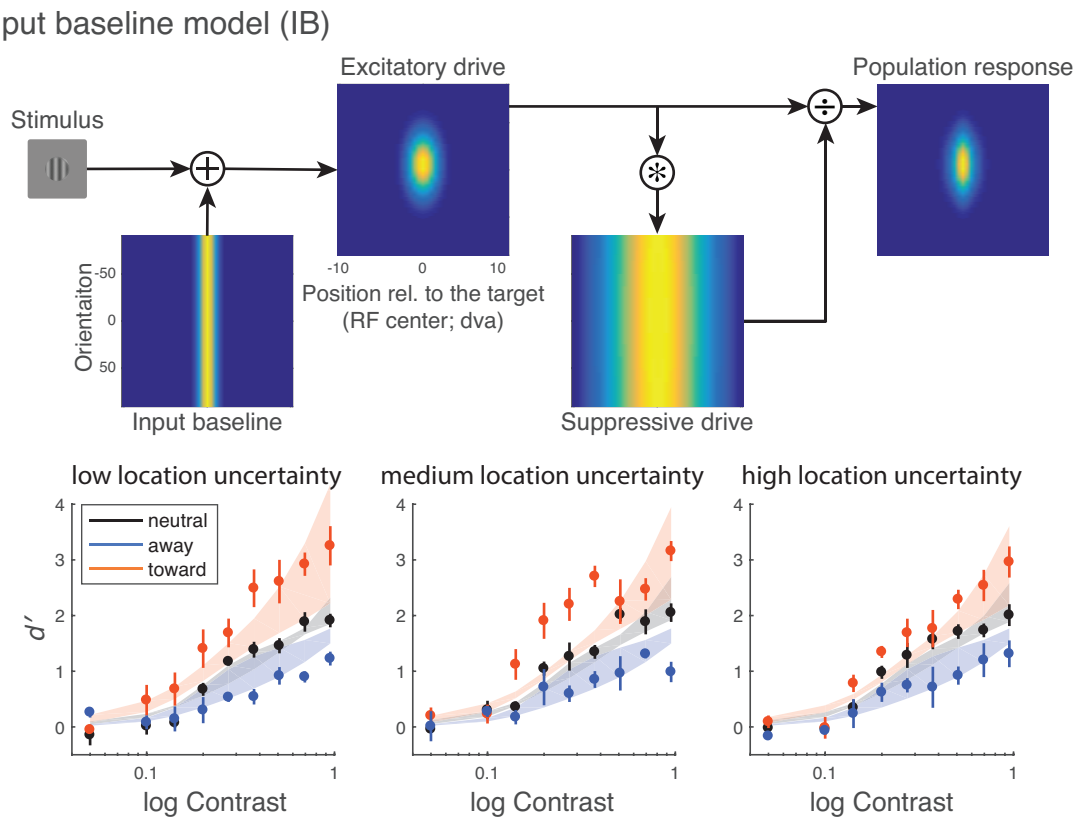

Supplementary Figure 8. Input baseline model and model fit. Top row: Input baseline model. Attentional modulation modeled as an additive term at the input baseline of the neuron. Bottom row: Model fit. Data points and error bars represent group-averaged data and ±1 s.e.m. The model was fitted to individual observers, and the shading areas represent the averaged of the fit across observers (mean ±1 s.e.m).

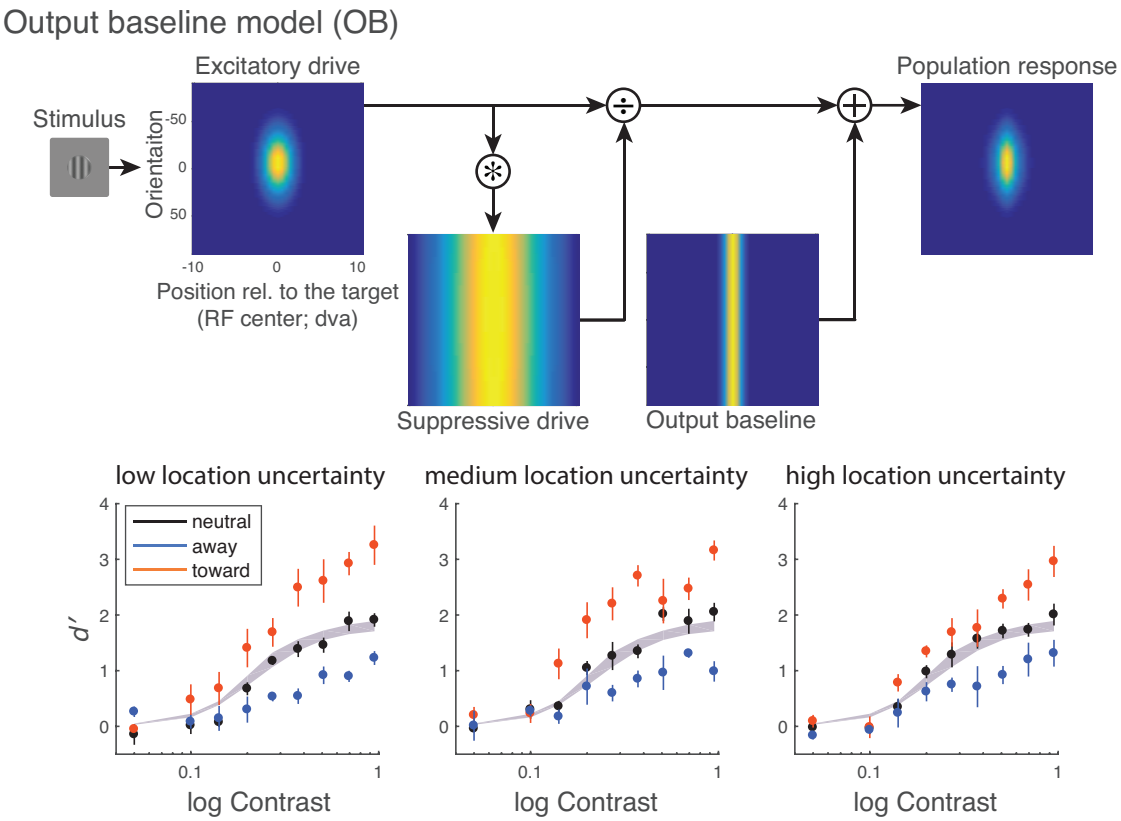

Supplementary Figure 9. **Output baseline model and model fit.** Top row: Output baseline model. Attention is modeled as an additive term after the normalization. Bottom row: Model fit. Data points and error bars represent group-averaged data and ±1 s.e.m. The model was fitted to individual observers, and the shading areas represent the averaged of the fit across observers (mean ±1 s.e.m). The model predicted that behavioral performance would be the same across the Neutral, Toward and Away conditions, and thus the shading areas of the three conditions overlap (bottom row).

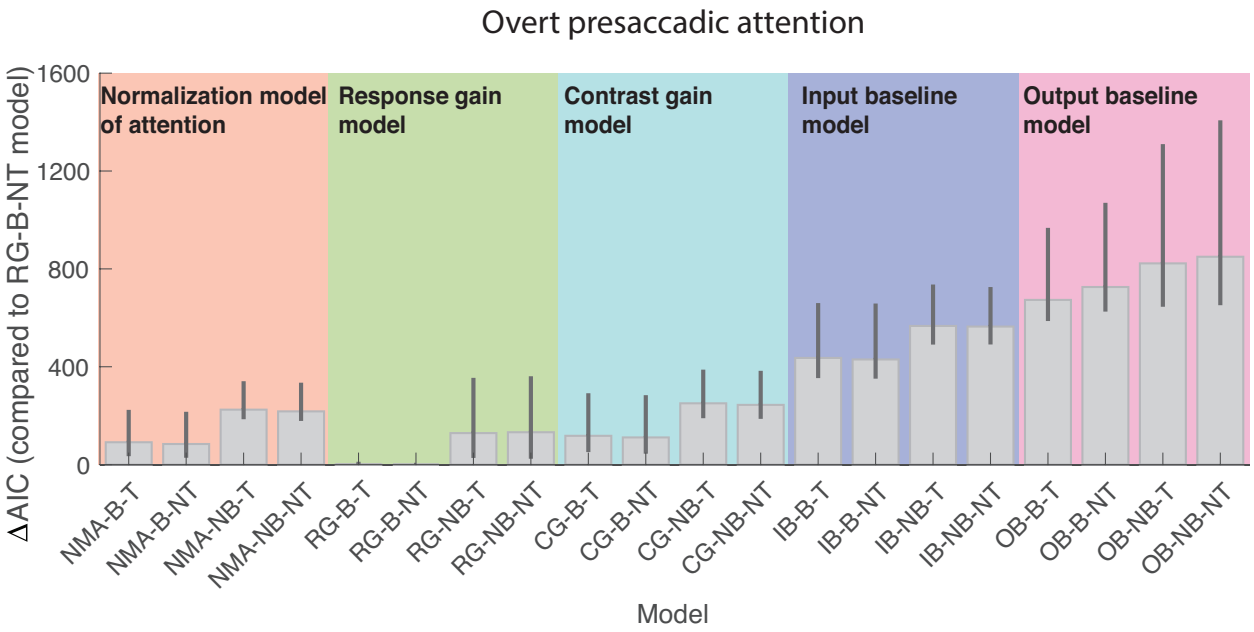

Supplementary Figure 10. **Factorial model comparison for overt presaccadic attention using AIC.** ΔAIC is the AIC of each model minus the AIC of the best-fit model (RG-B-NT). The bars represent ΔAIC summed across participants. The error bars represent 95% bootstrapped confidence interval. Names of the model are denoted as the attentional modulation paired with different implementations of other factors in the model separated by hyphens (-). NMA: normalization model of attention. RG: response gain; CG: contrast gain; IB: input baseline; OB: output baseline; B: response bias allowed; NB: no response bias allowed; T: trade-off between attention field size and the strength of attention allowed; NT: no trade-off between attention field size and the strength of attention allowed.

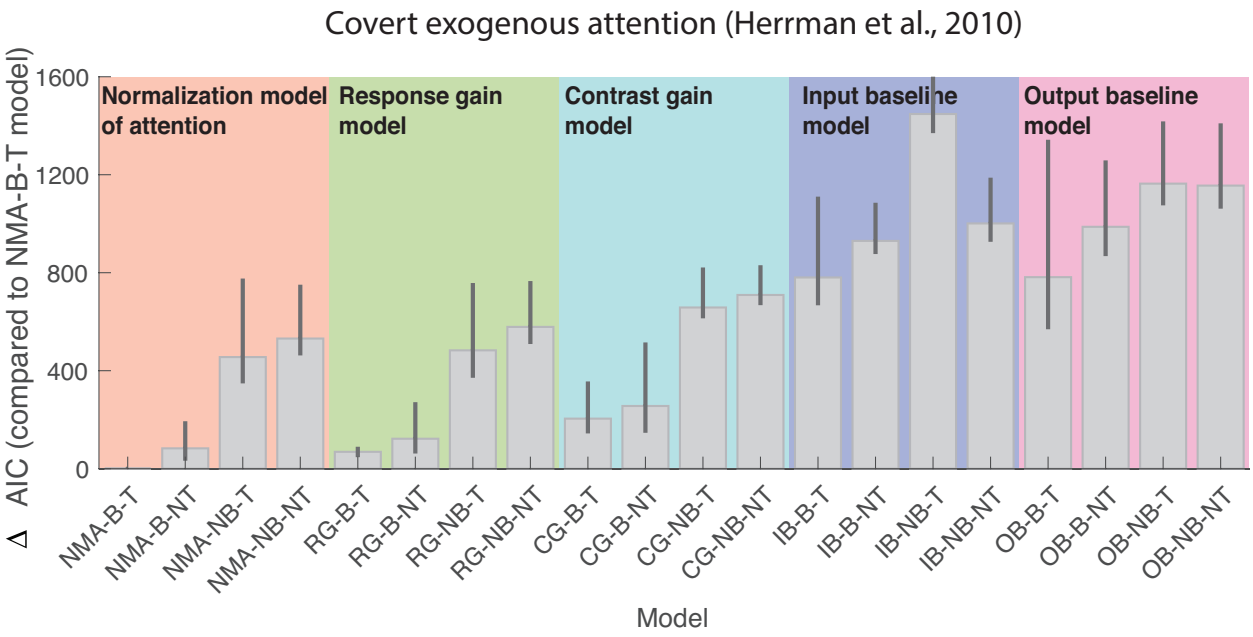

Supplementary Figure 11. **Factorial model comparison for covert exogenous attention using AIC.** ΔAIC is the AIC of each model minus the AIC of the best-fit model (NMA-B-T). The bars represent ΔAIC summed across participants. The error bars represent 95% bootstrapped confidence interval. Names of the model are denoted as the attentional modulation paired with different implementations of other factors in the model separated by hyphens (-). NMA: normalization model of attention. RG: response gain; CG: contrast gain; IB: input baseline; OB: output baseline; B: response bias allowed; NB: no response bias allowed; T: trade-off between attention field size and the strength of attention allowed; NT: no trade-off between attention field size and the strength of attention allowed.

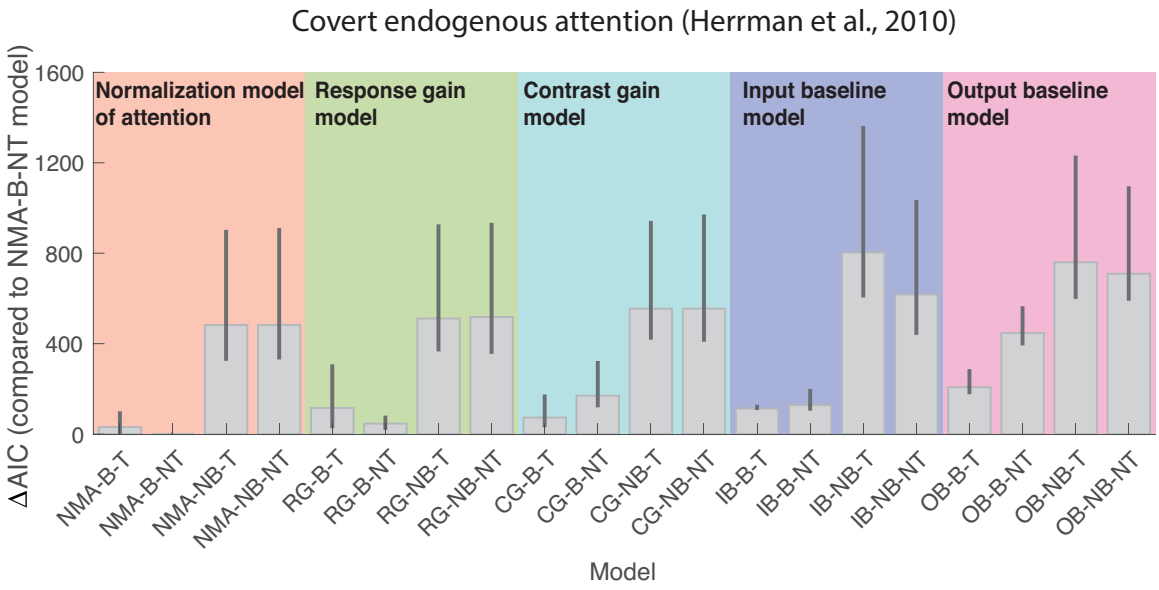

Supplementary Figure 12. **Factorial model comparison for covert endogenous attention using AIC.** ΔAIC is the AIC of each model minus the AIC of the best-fit model (NMA-B-NT). The bars represent ΔAIC summed across participants. The error bars represent 95% bootstrapped confidence interval. Names of the model are denoted as the attentional modulation paired with different implementations of other factors in the model separated by hyphens (-). NMA: normalization model of attention. RG: response gain; CG: contrast gain; IB: input baseline; OB: output baseline; B: response bias allowed; NB: no response bias allowed; T: trade-off between attention field size and the strength of attention allowed; NT: no trade-off between attention field size and the strength of attention allowed.

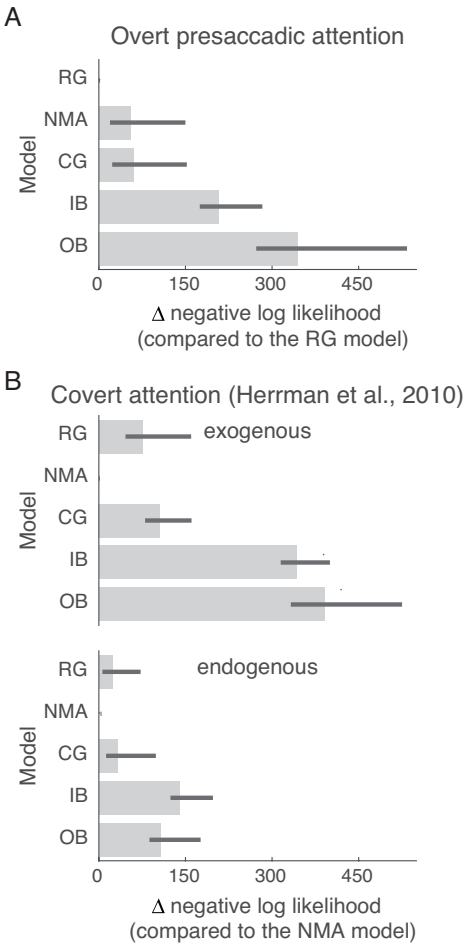

Supplementary Figure 13. Model comparison using cross-validated negative log-likelihood. (**A**) Model comparisons for the presaccadic attention experiments. The smaller the negative log-likelihood, the better the model performed in fitting the data. Δnegative log-likelihood is the negative log-likelihood of each model minus the negative log-likelihood of the best-fit model (response gain, RG, model). The bars represent Δnegative log-likelihood summed across participants. The error bars represent 95% bootstrapped confidence interval. (**B**) Model comparisons for the data reported in Herrmann et al., 2010. Δnegative log-likelihood is the negative log-likelihood of each model minus the negative log-likelihood of the best-fit model (NMA model). RG: response gain; CG: contrast gain; IB: Input baseline; OB: output baseline. Here, all the models contain a response bias term *c* as a free parameter, without a trade-off term *p*.

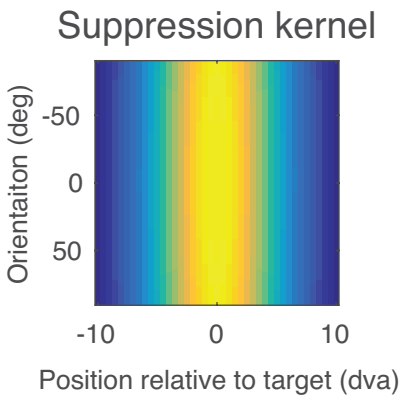

Supplementary Figure 14. Suppression kernel. The kernel used to convolve with the excitatory drive for computing the suppressive drive of the simulated neurons (*K* in equation 1).

Free parameters	Descriptions
σ	suppression constant of the neurons
n	exponent term of the neurons
σ_n	the magnitude of neural noise
w_n	the strength of attention in the neutral condition
w_t	the strength of attention in the Toward (or valid) condition
σ_{aL}	the width of attention field in the low uncertainty condition
σ_{aM}	the width of attention field in the medium uncertainty condition
σ_{aH}	the width of attention field in the high uncertainty condition
c	response bias
p	the trade-off between the strength of attentional modulation and the size of attentional field
All the models contain free parameters $\sigma, n, \sigma_n, w_n, w_t, \sigma_{aL}, \sigma_{aM}, \sigma_{aH}$. The other two parameters, *c* and *p*, were either set as a free paraemter or fixed at 0 depending whether the model allows a response bias, a trade-off term or both. The strength of attention in the Away condition was set at 0 as a baseline. The strength of attention in the Away (or invalid) condition was fixed at zero as the baseline. The width of attention field was constrained as $\sigma_{aL} <= \sigma_{aM} <= \sigma_{aH}$. Herrmann et al. (2010) only tested two levels of location uncertainty, and thus only two free parameters (σ_{aL}, σ_{aH}) were used for the width of attention field when fitting their data.	

Supplementary Table 1. Free parameters of the model.

Free parameters	O1	O2	O3	O4
σ	-2.44	-2.56	-1.94	-2.28
n	2.26	1.93	4.20	2.61
σ_n	1.96	2.05	2.10	1.92
w_n	1.51	3.50	2.79	2.28
w_t	3.28	9.42	5.05	4.28
σ_{aL}	0.81	1.67	4.31	0.35
σ_{aM}	1.86	1.67	4.31	1.82
σ_{aH}	1.86	2.48	4.31	3.01
c	0.06	0.17	0.02	-0.02

Supplementary Table 2. Best-fit free parameters of the response gain model for the overt presaccadic attention experiments. Best-fit parameters of the response gain model for individual participants in the overt presaccadic attention experiment (Figure. 7b). The values of σ and σ_n are fitted and reported in log scale.

Free parameters	O1	O2	O3	O4
σ	-2.70	-2.20	-1.82	-2.80
n	1.52	1.87	3.94	1.28
σ_n	1.71	1.64	1.89	1.47
w_n	4.51	11.22	10.36	4.39
w_t	12.35	77.55	44.12	10.17
σ_{aL}	0.01	0.41	0.25	0.01
σ_{aM}	1.29	1.01	0.25	3.30
σ_{aH}	1.52	1.65	1.91	3.30
c	0.06	0.17	0.03	-0.02

Supplementary Table 3. Best-fit free parameters of the normalization model of attention for the overt presaccadic attention experiments. Best-fit parameters of the NMA for individual participants in the overt presaccadic attention experiment (Figure. 7d). The values of σ and σ_n are fitted and reported in log scale.